ORIGINAL ARTICLE

Ozone-primed neutrophils promote early steps of tumour cell metastasis to lungs by enhancing their NET production

Natacha Rocks,[1] Céline Vanwinge,[1] Coraline Radermecker,[2,3] Silvia Blacher,[1] Christine Gilles,[1] Raphael Marée,[4] Alison Gillard,[1] Brigitte Evrard,[5] Christel Pequeux,[1] Thomas Marichal,[2,3,6] Agnes Noel,[1] Didier Cataldo[1,7]

► Additional material is published online only. To view please visit the journal online (http://dx.doi.org/10.1136/thoraxjnl-2018-211990).

For numbered affiliations see end of article.

Correspondence to
Professor Didier Cataldo, Laboratory of Tumor and Development Biology, GIGA Research Center, University of Liège and Departement of Respiratory Diseases, CHU Liège 4000, Belgium; didier.cataldo@uliege.be

Received 25 April 2018
Revised 21 March 2019
Accepted 10 April 2019
Published Online First 29 May 2019

ABSTRACT

Background Air pollution, including particulates and gazes such as ozone (O_3), is detrimental for patient's health and has repeatedly been correlated to increased morbidity and mortality in industrialised countries. Although studies have described a link between ambient particulate matter and increased lung cancer morbidity, no direct relation has yet been established between O_3 exposure and metastatic dissemination to lungs.

Objectives To outline the mechanisms through which pulmonary O_3 exposure modulates metastasis kinetics in an experimental mouse model of O_3 exposure.

Methods Metastatic responses to pulmonary O_3 exposure were assessed using a reliable experimental mouse model of concomitant pulmonary O_3 exposure and tumour cell injection. Roles of neutrophils in O_3-induced lung metastasis were highlighted using blocking anti-Ly6G antibodies; moreover, the implication of neutrophil extracellular traps (NETs) in metastatic processes was evaluated using *MRP8cre-Pad4lox/lox* mice or by treating mice with DNase I.

Results Pulmonary O_3 exposure strongly facilitates the establishment of lung metastasis by (1) Inducing a pulmonary injury and neutrophilic inflammation, (2) Influencing very early steps of metastasis, (3) Priming neutrophils' phenotype to release NETs that favour tumour cell colonisation in lungs. The ability of O_3-primed neutrophils to enhance lung colonisation by tumour cells was proven after their adoptive transfer in Balb/c mice unexposed to O_3.

Conclusions Pulmonary neutrophils induced by O_3 promote metastatic dissemination to lungs by producing NETs. These findings open new perspectives to improve treatment and prevention strategies in patients affected by metastatic diseases.

Key messages

What is the key question?

► Does pulmonary ozone exposure impact metastatic processes of tumour cells?

What is the bottom line?

► Mice exposed to ozone display increased neutrophil counts in lung parenchyma and airways. Those neutrophils are primed to further promote metastatic dissemination processes of various tumour cells to lungs by inducing neutrophil extracellular trap release.

Why read on?

► Unravelling cellular and molecular mechanisms linking air pollution and more precisely ozone exposure to pulmonary damage or metastatic colonisation is mandatory. We demonstrate here for the first time that pulmonary ozone exposure is linked to an increased metastatic burden, which is dependent on neutrophil presence and phenotype.

INTRODUCTION

Air pollution is a major environmental risk to health. Indeed, although a strong epidemiological link has been established between tobacco consumption and increased morbidity and mortality,[1] evidence now accumulates demonstrating that environmental pollutants are also potent risk factors to increase the burden of pathologies as various as respiratory and heart diseases or stroke (source: WHO). Hence, as radiation-induced lung damage promotes breast cancer lung metastasis,[2] one could imagine that atmospheric pollutants cause serious lung damage and thereupon affect the development of pulmonary pathologies. Accordingly, the highest lung cancer incidence has been recorded among patients living along highways and in industrial zones where workers are exposed to diesel exhaust.[3] The actions of air pollutants on lung damage and subsequent cancer progression have been addressed by Richters and Kuraitis, which already described in 1983 in an elegant in vivo mouse study, that NO_2 inhalation increases numbers of melanoma nodules in mouse lungs.[4] Notwithstanding the epidemiological evidence linking air pollution with cancer progression, mechanistic reports linking ozone (O_3) exposure to increased cancer cell dissemination to lung tissues are still scarce.

Neutrophils emerged as one of the most important key players linking indoor and outdoor pollutants to cancer development.[5] Hence, smokers suffering from COPD, a disease characterised by neutrophilic inflammation, develop significantly higher rates of lung cancer as compared with people who smoked the same amount of tobacco without developing COPD and COPD-related neutrophilic pulmonary inflammation.[6 7]

To cite: Rocks N, Vanwinge C, Radermecker C, *et al*. *Thorax* 2019;**74**:768–779.

Although neutrophils display both protumour and antitumour functions, many studies focused on their protumour properties. Hence, neutrophils can drive oncogenic transformation and support tumour cell survival, proliferation and resistance to chemotherapy.[8] Moreover, neutrophils promote the metastatic cascade by stimulating tumour cell migration and invasion and, by clustering around tumour cells, protect them from immune surveillance.[8–10] Treatment strategies consisting of systemically targeting neutrophils in patients to reduce metastatic burden are causing severe neutropenia, thus jeopardising patient's health by causing infections. Therefore, cellular and molecular mechanisms linking neutrophils to cancer development and progression should be more thoroughly explored. Recent studies have identified that extracellular DNA meshes produced by neutrophils, also called NETs (for neutrophil extracellular traps), are involved in metastatic dissemination processes by awakening dormant cancer cells,[11] 'trapping' circulating cancer cells, enhancing vascular permeability or inducing cell invasion.[12] NETs, whose formation and release depends, in most outlines, on neutrophil elastase, myeloperoxidase and peptidylarginine deiminase 4 (Pad4), are made of abundant chromatin fibres bearing citrullinated histones as well as of proteins issued from primary, secondary or tertiary neutrophil granules.[13 14]

In this work, we demonstrate, using a reliable experimental mouse model of concomitant pulmonary ozone exposure and tumour cell injection, that ozone exposure causes increased tumour cell colonisation to lung tissues. The importance of ozone-induced neutrophils in metastatic burden is supported by the significantly decreased lung metastasis observed on neutrophil blockade. By using neutrophil-restricted *Pad4*-deficient mice and NET-degrading DNAse, we demonstrate here that ozone primes neutrophils to produce NETs, which influence early metastatic processes.

METHODS

Details are provided in the online supplementary material and methods section.

Statistics

Data are reported in a box plot where median values are presented as a horizontal middle line and the IQR by upper and lower horizontal lines. In vitro cell proliferation rates are presented as bar graphs where bars represent median values and upper and lower horizontal lines represent the IQR. Statistical differences were assessed between experimental groups using Wilcoxon, Mann-Whitney or Kruskal-Wallis tests (GraphPad Prism).

Data related to the kinetics of primary tumour development are reported as median values with IQRs, where the median values are calculated based on the mean primary tumour volumes measured on each left and right primary tumour *per* mouse. A statistical evaluation (Mann-Whitney test) determining whether air-exposed or ozone-exposed groups display differences in primary tumour volumes has been performed on each time point of tumour volume measurement (two experimental groups, five measurements over time). In addition, a non-parametrical two-sample Kolmogorov-Smirnov test (K-S test) was used to determine if two curves follow the same distribution over time.

Asterisks indicate comparisons of specific experimental conditions with statistical significance (*p<0.05; **p<0.01; ***p<0.001).

RESULTS

Ozone exposure induces a pulmonary neutrophilic inflammation

To evaluate the impact of ozone on lung tissues, mice were exposed to 2 ppm ozone during 3 hours per day for three consecutive days and sacrificed on day 4 (figure 1A). Total protein contents, measured in bronchoalveolar lavage fluids (BALFs) and reflecting pulmonary damage, were higher in mice challenged with ozone as compared with mice exposed to control air (*p<0.05, n=10) (figure 1B). Bronchial wall inflammation was increased in mice exposed to ozone (***p<0.001, n=10) (figure 1C) and differential cell counts performed on inflammatory cells present in bronchoalveolar lavages (BAL) showed higher neutrophil counts in ozone-challenged animals (6.34±2.05 *vs* 133.70±28.09 (*10^3 cells/mL) in air vs ozone-challenged animals; ***p<0.001, n=10) (figure 1D). The profile of ozone-induced inflammation in lungs was confirmed using flow cytometry. $CD45^+$ cells isolated from lung tissues were stained with antibodies to identify subtypes of granulocytes, lymphocytes and monocytes. Among all analysed cells, neutrophils ($GR1^+$, $Ly6B.2^+$) were thoroughly elevated in lungs of ozone-treated mice (**p<0.01, n=10 (air), n=9 (ozone)) (figure 1E–F). Moreover, higher dextran density was measured in lung parenchyma of ozone-treated mice (p=0.1775, n=5 (air), n=6 (ozone)) (figure 1G–H) indicating that the permeability of pulmonary vasculature was enhanced. This finding is supported by measuring higher albumin levels in BALF of ozone-exposed mice (**p<0.01, n=8) (figure 1I).

Altogether these results show that ozone exposure provokes an increased pulmonary inflammation, mainly composed of neutrophils, and a pulmonary injury linked to an increased vascular permeability.

Pulmonary ozone exposure increases lung tissue colonisation by tumour cells

Using a reliable experimental metastasis mouse model, we sought to determine the impact of ozone on lung tissue colonisation by tumour cells. Mice were exposed for three consecutive days to ozone and then subjected to an intravenous injection of 4T1 mammary tumour cells. Ozone exposure was pursued every second weekday (days 5, 8 and 10 of the experimental set-up) until biophotonic imaging and sacrifice (figure 2A). Interestingly, the increased pulmonary neutrophilic inflammation observed on ozone exposure (**p<0.01, n=15) (figure 2B) was associated with increased lung colonisation by 4T1 tumour cells as demonstrated by bioluminescent imaging and tumour area quantification on H&E-stained histological lung sections (*p<0.05, n=15) (figure 2C–E). The increased tumour cell dissemination to lung parenchyma following ozone exposure was also demonstrated by using mouse B16K1 melanoma cells. In this assay, mice were sacrificed 26 days after B16K1 cell injection, when metastatic foci were well developed and could be quantified on histological slides (figure 2F). Again, ozone exposure induced a neutrophilic recruitment to lung tissues (figure 2G) and B16K1 colonisation in lungs was strongly enhanced (***p<0.001, n=10) (figure 2H–I).

The impact of ozone on the entire metastatic cascade was further proven using a spontaneous metastasis mouse model among which air-challenged or ozone-challenged mice were subcutaneously injected with 4T1 cells (figure 2J). While no difference in primary tumour volume kinetics could be noted (p=0.99) (figure 2K), a significant increase in 4T1 metastatic dissemination to lungs was observed in the ozone-treated

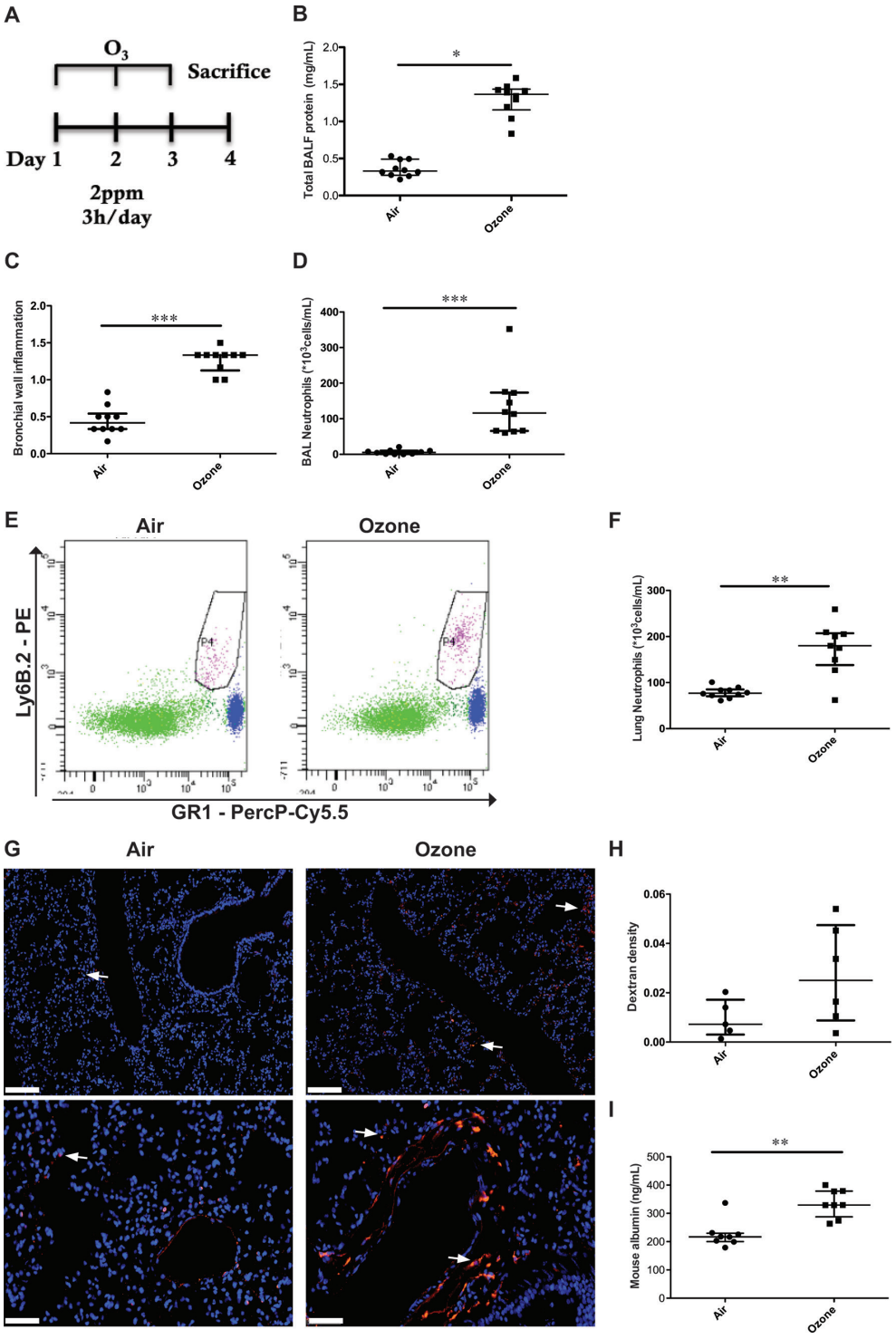

Figure 1 Ozone exposure induces lung neutrophilic inflammation, pulmonary injury and alters vessel permeability. (A) Timeline of ozone exposure. Mice are exposed to ozone (O_3) or air for three consecutive days (2 ppm O_3; 3 hours per day) and are sacrificed on day 4 of the experimental set-up. (B) Total protein levels are measured in bronchoalveolar lavage fluids (BALF) of mice exposed to air or ozone. (C) Bronchial wall inflammation assessed on H&E-stained histological lung tissue slides. (D) Neutrophil numbers present in bronchoalveolar lavages (BAL). (*p<0.05; ***p<0.001; Mann-Whitney test). Error bars represent the IQR; n=10. (E) Flow cytometry dot plots of GR1-labelled and Ly6B.2-labelled cells. $GR1^+$ and $Ly6B2^+$ neutrophils are identified in selected windows (P4). (F) Graphic representation of lung neutrophil numbers in air or ozone-treated mice. **p<0.01; Mann-Whitney test). Error bars represent the IQR; n=9 in ozone, n=10 in the air-treated group. (G) Representative photographs of lung tissues from mice exposed to air or ozone and intravenously injected with rhodamin-dextran (red, marked by white arrows) to identify vascular leakage (upper panel – scale bar: 500 µm; lower panel – scale bar: 50 µm). (H) Computer-assisted quantification of vascular leakage (dextran density) in air, or ozone-exposed lungs (p=0.1775). Results are expressed as median dextran density, where each dot represents the mean dextran value obtained from two histological sections analysed per sample, taken at different sites of the lung. Error bars represent the IQR; n=5 mice in air, n=6 mice in the ozone-treated group. (I) Albumin levels were quantified in BALF of air or ozone-challenged mice. (**p<0.01; Mann-Whitney test). Error bars represent the IQR; n=8 mice/experimental group. All results are representative of at least two experiments performed individually.

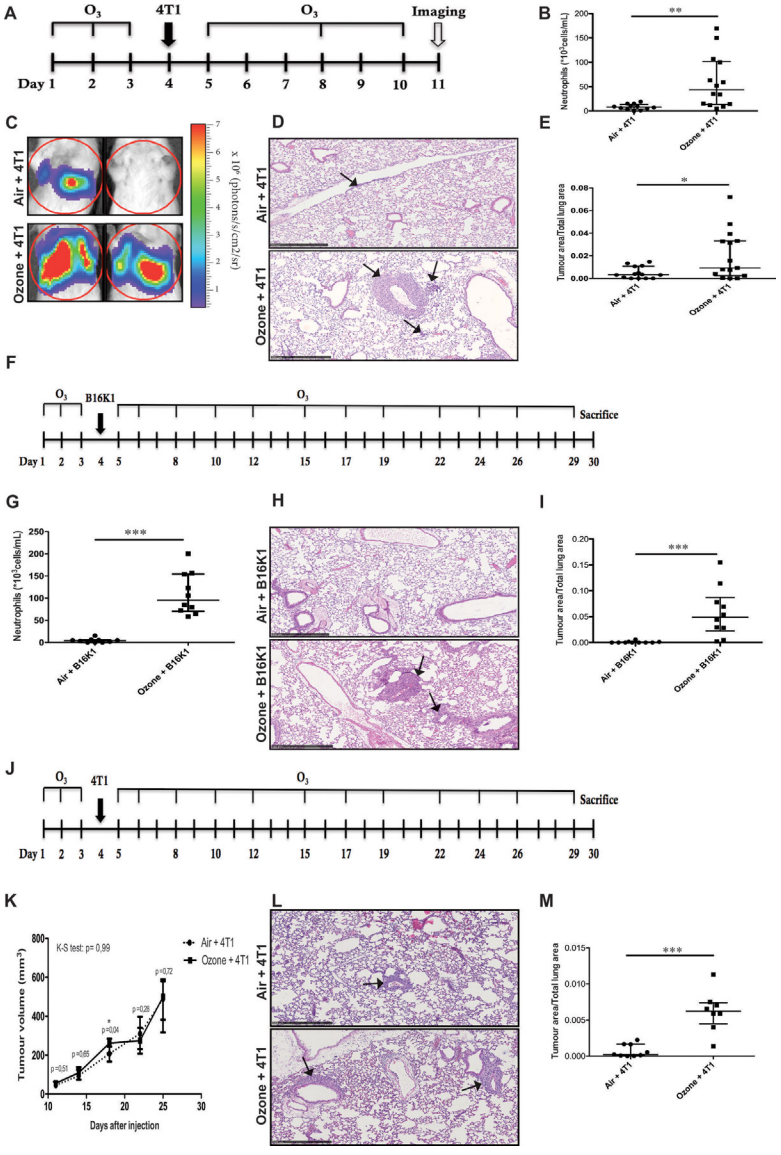

Figure 2 Ozone exposure induces tumour cell metastasis to lung tissues. (A) Timeline of ozone (O_3) exposure and intravenous mammary 4T1 tumour cell injection (black arrow). Upper bars represent the days of ozone exposure. After three consecutive days of ozone challenge, 4T1 cells were intravenously injected on day 4 and ozone exposure was sustained every second weekday (days 5, 8, 10) until the end of the experiment. Tumour cell colonisation to lung tissues was imaged at day 11 using the in vivo imaging system (IVIS) Xenogen IVIS 200 (white arrow) (n=15). (B) Bronchoalveolar lavage (BAL) neutrophil counts in mice exposed or not (air) to ozone and intravenously injected with 4T1 cells. (C) Biophotonic monitoring of regions of interest (lungs, red circles) in mice exposed to air or ozone and injected with luciferase-transfected 4T1 cells. Images have been taken in 'photon mode' and are representative of all mice. (D) Representative H&E-stained lung tissue sections of mice exposed to air or ozone and intravenously injected with 4T1 cells. Black arrows mark tumour islets. Scale bar: 500 µm. (E) Tumour area quantification on five histological slides per mouse lung. Results are expressed as a ratio of tumour area and total area of lung tissue analysed. (*p<0.05; **p<0.01; Mann-Whitney test). Error bars represent the IQR; n=15 mice/experimental group. These results are representative of at least two experiments. (F) Timeline of ozone (O_3) exposure and intravenous B16K1 melanoma cell injection (black arrow). Upper bars represent the days of ozone exposure. Mice were sacrificed 26 days after B16K1 tumour cell injection (n=10). (G) Neutrophil numbers in BAL of mice exposed to air or ozone and intravenously injected with B16K1 cells. (H) Representative H&E-stained lung tissue sections of mice exposed to air or ozone and intravenously injected with B16K1 cells. Black arrows mark tumour islets. Scale bar: 500 µm. (I) Tumour area quantification is calculated on five slides per mouse lung by reporting tumour area to total lung tissue area. (***p<0.001; Mann-Whitney test). Error bars represent the IQR; n=10 mice/experimental group. These results are representative of at least two experiments performed individually. (J) Timeline of ozone (O_3) exposure and subcutaneous 4T1 mammary cell injection (black arrow). Upper bars represent the days of ozone exposure. Mice were sacrificed 26 days after subcutaneous 4T1 tumour cell injection (n=8–9). (K) Primary tumour volumes were calculated on a regular basis in air-treated or ozone-treated animals until sacrifice. Statistical differences between experimental groups were assessed at each time point. Results are expressed as median±IQR (*p<0.05; Mann-Whitney test). Primary tumour growth kinetics of both experimental groups were analysed using Kolmogorov-Smirnov test (p=0.99). (L) Representative histological H&E images where black arrows show tumour islets in lung tissues. Scale bar: 500 µm. (M) Metastatic dissemination of mammary tumour cells was evaluated by measuring the ratio of area occupied by tumour islets in lung tissues and total lung tissue area, on five slides per each mouse lung. (***p<0.001; Mann-Whitney test). Results are expressed as median±the IQR; n=8 (ozone +4T1), n=9 (air +4T1) mice/experimental group. Results are representative of two experiments performed individually.

group (***p<0.001, n=8 (ozone +4T1), n=9 (air +4T1)) (figure 2L–M).

Taken together, these results demonstrate that inhaled ozone promotes tumour cell metastasis to lungs.

Ozone exposure accelerates early steps of tumour cell metastasis to lungs

In order to verify whether ozone exposure impacts on early metastatic steps, tumour cell arrest in lungs was monitored 30 min, 2 hours, 24 hours or 48 hours after intravenous 4T1 tumour cell injection (figure 3A). Remarkably, an increased 4T1-related bioluminescence was quantified in ozone-exposed lungs already 30 min after tumour cell injection (504 000 *vs* 902 000 photons/s/cm^2/sr in air-exposed versus ozone-exposed lungs, p=0.1508, n=5). This increased bioluminescence was also observed in other ozone-exposed experimental groups monitored either 2 hours (p=0.4206, n=5), 24 hours (*p<0.05, n=15) or 48 hours after 4T1 injection (***p<0.001, n=10) (figure 3B–G). To further confirm results obtained by bioluminescent imaging, CMTPX-labelled 4T1 cells were intravenously injected into air-exposed or ozone-exposed mice. Forty-eight hours later, numbers of extravasated 4T1 cells were significantly higher in the ozone-exposed lung parenchyma (**p<0.01, n=5) (figure 3H–I).

To extend our observations on another tumour cell type, experiments were reiterated using NOD-Scid or Balb/cJRj mice, exposed to ozone and subsequently intravenously injected with luciferase-expressing MDA-MB-231 cells (Human mammary tumour cell line isolated at MD Anderson Cancer Center from a pleural effusion of a patient bearing invasive ductal carcinoma) (figure 4A, online supplementary figure 1A). Tumour cell-related luciferase activity was clearly higher in ozone-treated lungs at an early time point after injection (24 hours), independently of mouse strain used (***p<0.001, n=9–10) (figure 4B–C, online supplementary figure 1B-C). These data clearly demonstrate that ozone exposure impacts early steps of lung colonisation by tumour cells. Interestingly, the increased lung colonisation by MDA-MB-231 tumour cells following ozone exposure was also maintained at later time points (7 days (*p<0.05) and 28 days (**p<0.01) after MDA-MB-231 intravenous injection, day 11 and day 32 of the experimental set-up, respectively) (n=9–10) (figure 4D–G).

Neutrophil depletion reverses the effects of ozone on tumour cell colonisation in lung tissues

To evaluate the importance of ozone-generated neutrophils in metastatic processes, anti-Ly6G antibodies (grey arrows) were used to deplete neutrophils in ozone-exposed lungs (figure 5A). As expected, anti-Ly6G antibody treatment strongly reduced ozone-induced lung neutrophilic inflammation (**p<0.01, n=9–10) (figure 5B). Short-term experiments combining ozone exposure, anti-Ly6G or control IgG treatment (days 1 and 4 of the experimental set-up) and intravenous 4T1 tumour cell injection (day 4) were implemented to assess neutrophils' contribution to early colonisation processes of 4T1 tumour cells. Remarkably, bioluminescence related to 4T1 cells was significantly decreased in animals concomitantly treated with ozone and anti-Ly6G antibodies 24 hours after 4T1 tumour cell injection (**p<0.01, n=5) (figure 5C–D). Neutrophil depletion also reduced metastatic development in lungs as shown in mice sacrificed 7 days after intravenous 4T1 injection (**p<0.01, n=9–10) (figure 5E–G). These data confirm our hypothesis of an implication of ozone-induced neutrophils in early metastatic events.

To corroborate results of depletion experiments performed with anti-Ly6G antibodies suggesting an implication of neutrophils in early ozone-induced metastatic events, an adoptive transfer of neutrophils was performed, for which neutrophils were extracted from ozone-treated or air-treated lungs, further instilled into naive mice and their implication on 4T1 recruitment to lungs was measured. Strikingly, instillation of neutrophils derived from ozone-treated lungs (PNN Ozone) led to increased pulmonary 4T1 colonisation as demonstrated by bioluminescent activity, attesting for their higher potential to favour tumour cell colonisation to lungs (**p<0.01, n=6) (figure 5H–I). These experiments were repeated using culture medium conditioned by neutrophils (previously isolated from ozone-treated or air-treated lungs) and generated very similar results (**p<0.01, n=6) (figure 5J–K).

Media conditioned by air-challenged or ozone-challenged neutrophils did however not affect in vitro 4T1 cell proliferation, migration or adhesion to a confluent SVEC (SV40-transformed mouse lymphoid vascular endothelial cells) monolayer (online supplementary figure 2).

These observations state for the first time that ozone exposure increases neutrophil counts in lung tissues, and primes neutrophils to produce different soluble factors, which influence tumour cell dissemination.

Ozone-primed neutrophils produce NETs

Activated neutrophils are able to release DNA filaments and protein contents from their granules, which form a network of extracellular fibres, known as NETs. NET production was first measured in our experimental mouse models by quantifying dsDNA levels in BALFs. Mice exposed to ozone displayed increased dsDNA levels in BAL fluids when compared with control animals (**p<0.01, n=6) (figure 6A). When exposed to ozone and injected with tumour cells (4T1, B16K1 or MDA-MB-231), mice systematically displayed increased dsDNA levels in BAL fluids, and this already 24 hours after tumour cell injection (*p<0.05; **p<0.01, n=6) (figure 6A). Interestingly, dsDNA levels were decreased when neutrophil recruitment was inhibited using anti-Ly6G antibody (Ozone +4T1+anti-Ly6G, *p<0.05, n=9–10) (figure 6B). Culture media conditioned by ex vivo cultured ozone-stimulated neutrophils also displayed higher dsDNA levels when compared with control media conditioned by air-stimulated neutrophils (Air) (**p<0.01, n=6) (figure 6C) attesting that dsDNA release observed in the metastasis models is specific of neutrophils. Ex vivo treatment of ozone-stimulated neutrophils with specific inhibitors of NET development (Pad4i or DNase I) drastically reduced dsDNA levels in culture media (**p<0.01, n=6) (figure 6C). Consistent with results measuring dsDNA levels in BALF, Hoechst staining unveiled that ozone-stimulated neutrophils produced more NETs as compared with control neutrophils. Ex vivo stimulation of neutrophils with PMA (phorbol 12-myristate 13-acetate) promoted even more NET extensions in ozone-challenged neutrophils as shown by length cell density quantification (**p<0.01, n=6) (figure 6D–E). NET formation was further identified by immunofluorescence where cellular extensions double-positive for DNA (Hoechst staining, blue) and citrullinated histone H3 (CIT H3, red) were considered as NETs (white arrows). Again, ozone-stimulated neutrophils were able to produce more NETs in culture when compared with control neutrophils, while Pad4i considerably diminished ozone-induced NETs (figure 6F). NET

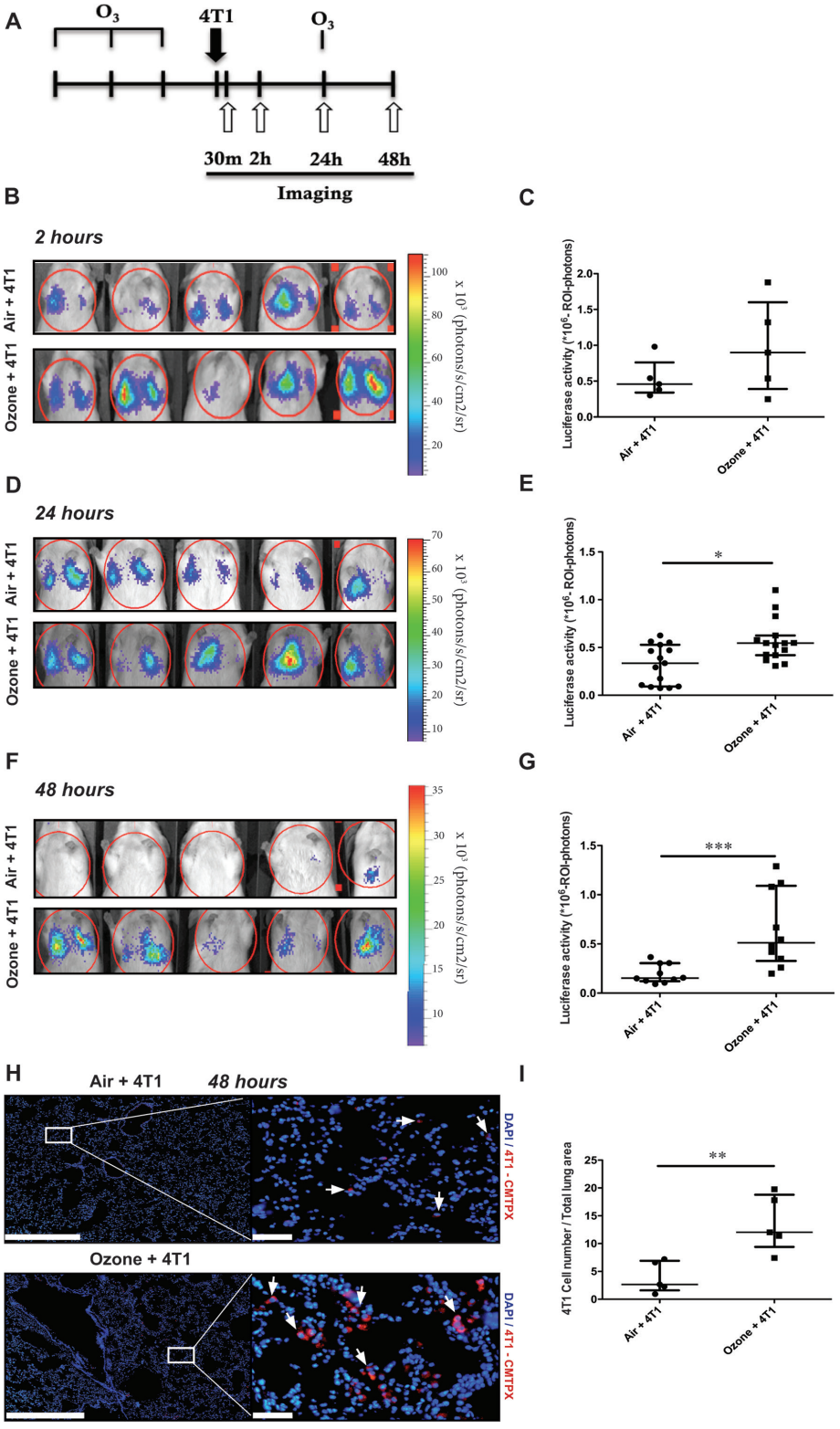

Figure 3 Ozone accelerates early tumour cell implantation in lung tissues. (A) Timeline of ozone exposure (O_3), intravenous 4T1 tumour cell injection (black arrow) and short-term imaging of tumour cell arrival in lungs, 30 min, 2 hours, 24 hours or 48 hours after tumour cell injection (white arrows). (B–G) Biophotonic imaging (photon mode) of luciferase activity related to 4T1 tumour cells in lungs of mice (red circles) exposed to ambient air or ozone. Images were taken 2 hours (B), 24 hours (D) or 48 hours (F) after tumour cell injection. Corresponding bioluminescence quantification of regions of interest (ROI) in lungs is shown in the right panels (2 hours (p=0.4206) (C), 24 hours (E), 48 hours (G)). (*p<0.05; ***p<0.001; Mann-Whitney test). Error bars represent the IQR; n=5 (2 hours), n=15 (24 hours) or n=10 (48 hours) mice/experimental group. Results are representative of two experiments performed individually. (H) Representative photographs of lung tissues from mice exposed to air or ozone and intravenously injected with CMTPX red-labelled 4T1 tumour cells. White arrows mark red tumour cells. Right panel (scale bar: 50 µm) is a zoom of the left panel (scale bar: 500 µm). (I) Quantification of red-labelled 4T1 cells counted in lung tissues of air-exposed or ozone-exposed mice. (**p<0.01; Mann-Whitney test). Bars represent the IQR, n=5 mice/experimental group.

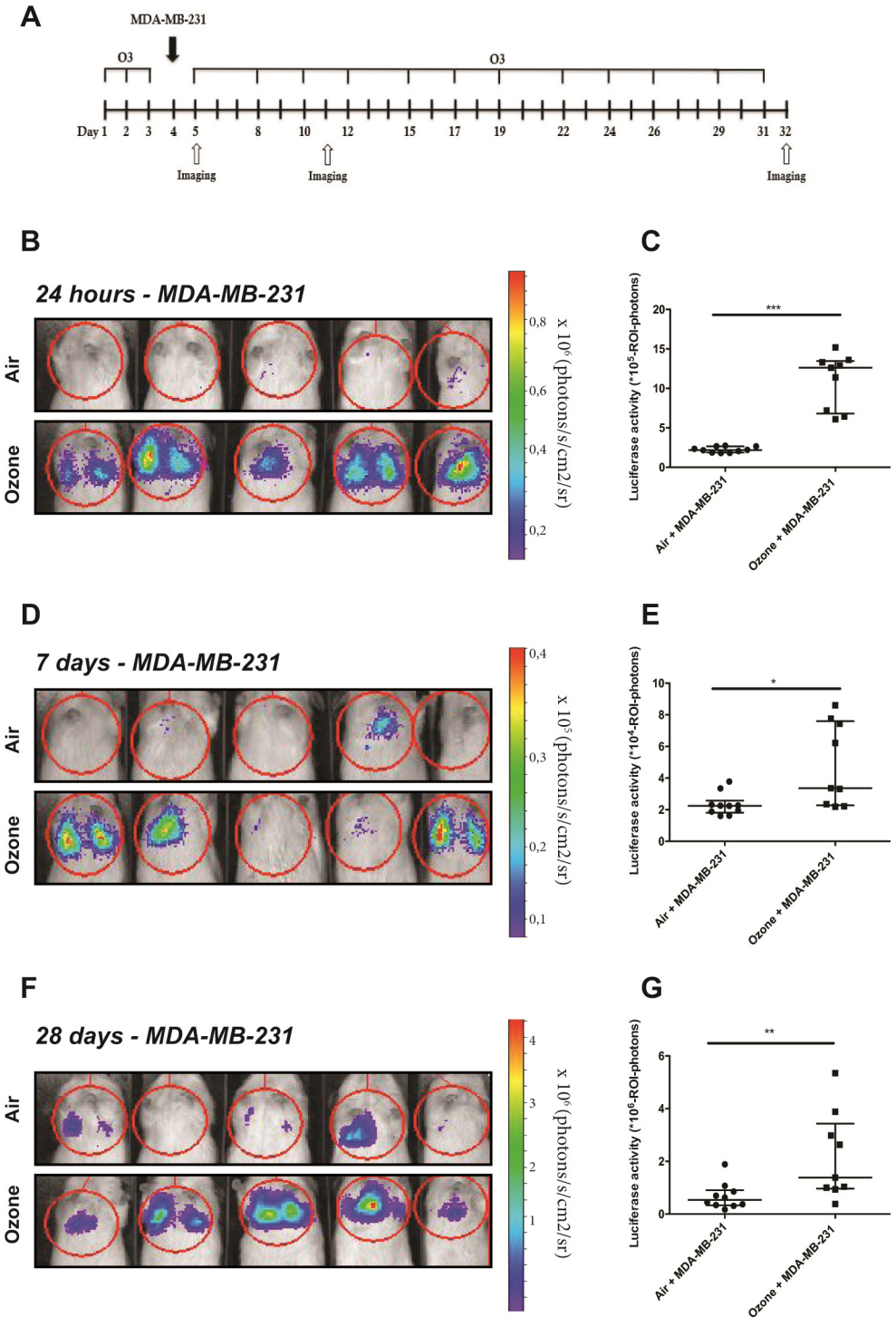

Figure 4 Ozone impacts colonisation of MDA-MB-231 mammary tumour cells to lungs. (A) Timeline of a 3-day ozone exposure followed by an intravenous MDA-MB-231 cell injection (black arrow). Upper bars represent the days of ozone exposure (every second weekday until the end of the experiment). The presence of tumour cells in lungs was monitored 24 hours, 7 days and 28 days after MDA-MB-231 injection (white arrows) (days 5, 11 and 32 of the experimental set-up, respectively). (B–G) Representative images of MDA-MB-231-related luciferase imaging (photon mode) in lungs of mice (red circles) exposed to air or ozone, taken 24 hours (B), 7 days (D) and 28 days (F) after intravenous MDA-MB-231 cell injection. (C–G) Luciferase activity was quantified in regions of interest (ROI) determined around lungs in mice treated with air or ozone, 24 hours (C), 7 days (E) and 28 days (G) after intravenous MDA-MB-231 cell injection. (*p<0.05; **p<0.01; ***p<0.001; Mann-Whitney test). Error bars represent the IQR; n=9–10 mice/experimental group.

structures, double-positive for citrullinated histone 3 and MPO staining (specific of NETs), could also be identified on lung tissue sections of ozone-challenged mice (figure 6G). Higher levels of citrullinated histone 3 were detected by western blot in protein extracts of ozone-exposed lungs, confirming the enhanced presence of NETs (**p<0.01, n=7) (figure 6H).

Notably, ELISA measurements showed elevated CXCL1, CXCL2 and G-CSF (granulocyte colony-stimulating factor) levels

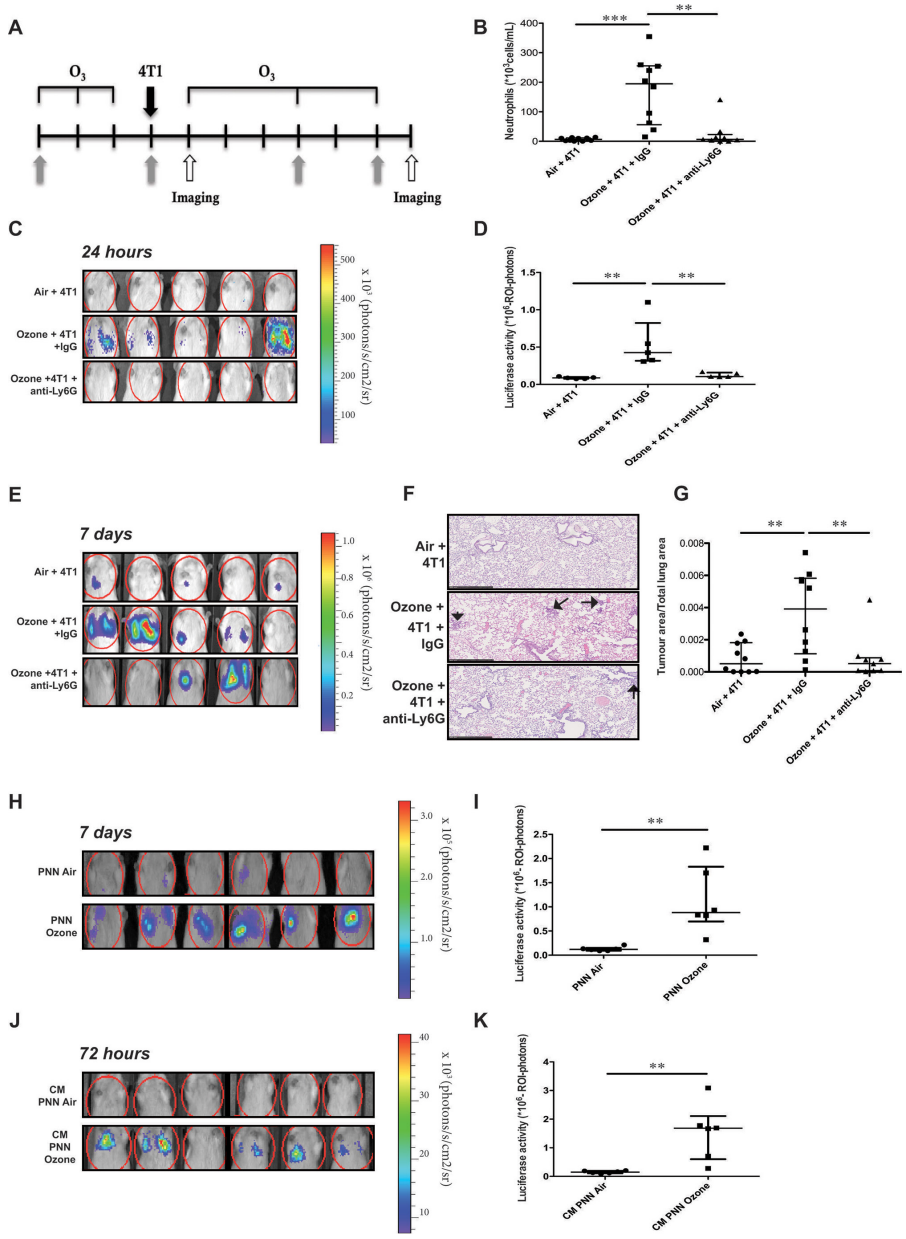

Figure 5 Neutrophil depletion reduces ozone-induced pulmonary tumour cell colonisation. (A) Timeline representing the experimental protocol of ozone (O_3) exposure and intravenous tumour cell injection (4T1, black arrow). After three consecutive days of ozone treatment, 4T1 cells were intravenously injected and ozone exposure was sustained every second weekday (days 5, 8, 10 of the experimental set-up) until the end of the experiment. Anti-Ly6G or control antibodies were intraperitoneally administered on days 1, 4, 8 and 10 (grey arrows) and tumour cell arrival in lungs was monitored on days 5 and 11 of the protocol (white arrows) corresponding respectively to 24 hours (n=5) and 7 days (n=9–10) after intravenous tumour cell injection. (B) Neutrophil counts in bronchoalveolar lavage (BAL) from mice injected with 4T1 cells and exposed to air (air+4T1) or ozone and treated or not with anti-Ly6G antibodies (Ozone +4T1+anti-Ly6G; ozone +4T1+IgG, respectively) (**p<0.01; ***p<0.001; Mann-Whitney test). Error bars represent the IQR; n=9 (ozone +4T1+anti-Ly6G), 10 mice/experimental group. These results represent two experiments performed individually. (C) Biophotonic imaging of tumour cell-related luciferase activity in regions of interest (ROI, red circles) 24 hours after 4T1 intravenous injection. Images shown have been taken in 'photon mode' and are representative of all mice analysed. (D) Quantification of luciferase activity (photons) in ROI (**p<0.01; Mann-Whitney test). Bars represent the IQR; n=5 mice/experimental group. (E) Biophotonic imaging of luciferase activity of tumour cells in ROI (red circles) 7 days after intravenous 4T1 injection. Images shown have been taken in 'photon mode' and are representative of all mice analysed. (F) Representative H&E-stained histological lung slides. Black arrows show tumour islets in lung tissues. Scale bar: 500 µm. (G) Tumour area in lungs was quantified by measuring the ratio between tumour foci area and total area of analysed lungs. (**p<0.01; Mann-Whitney test). Error bars represent the IQR; n=9 (Ozone +4T1+anti-Ly6G), 10 mice/experimental group. These results represent two experiments performed individually. (H) Representative images of biophotonic luminescence measurements in lungs of mice (red circles) instilled with neutrophils derived from control air-treated (PNN Air) or ozone-treated lungs (PNN Ozone). (I) Quantification of luciferase activity in ROI (photon mode). (**p<0.01; Mann-Whitney test). Bars represent the IQR; n=6 mice/experimental group. (J) Representative images of biophotonic luminescence measurements in lungs of mice (red circles) instilled with media conditioned by neutrophils previously isolated from control air-treated (CM PNN Air) or ozone-treated lungs (CM PNN Ozone). (K) Quantification of luciferase activity in ROI (photon mode) (**p<0.01; Mann-Whitney test). Bars represent the IQR; n=6 mice/experimental group. PNN, polymorphonuclear neutrophil.

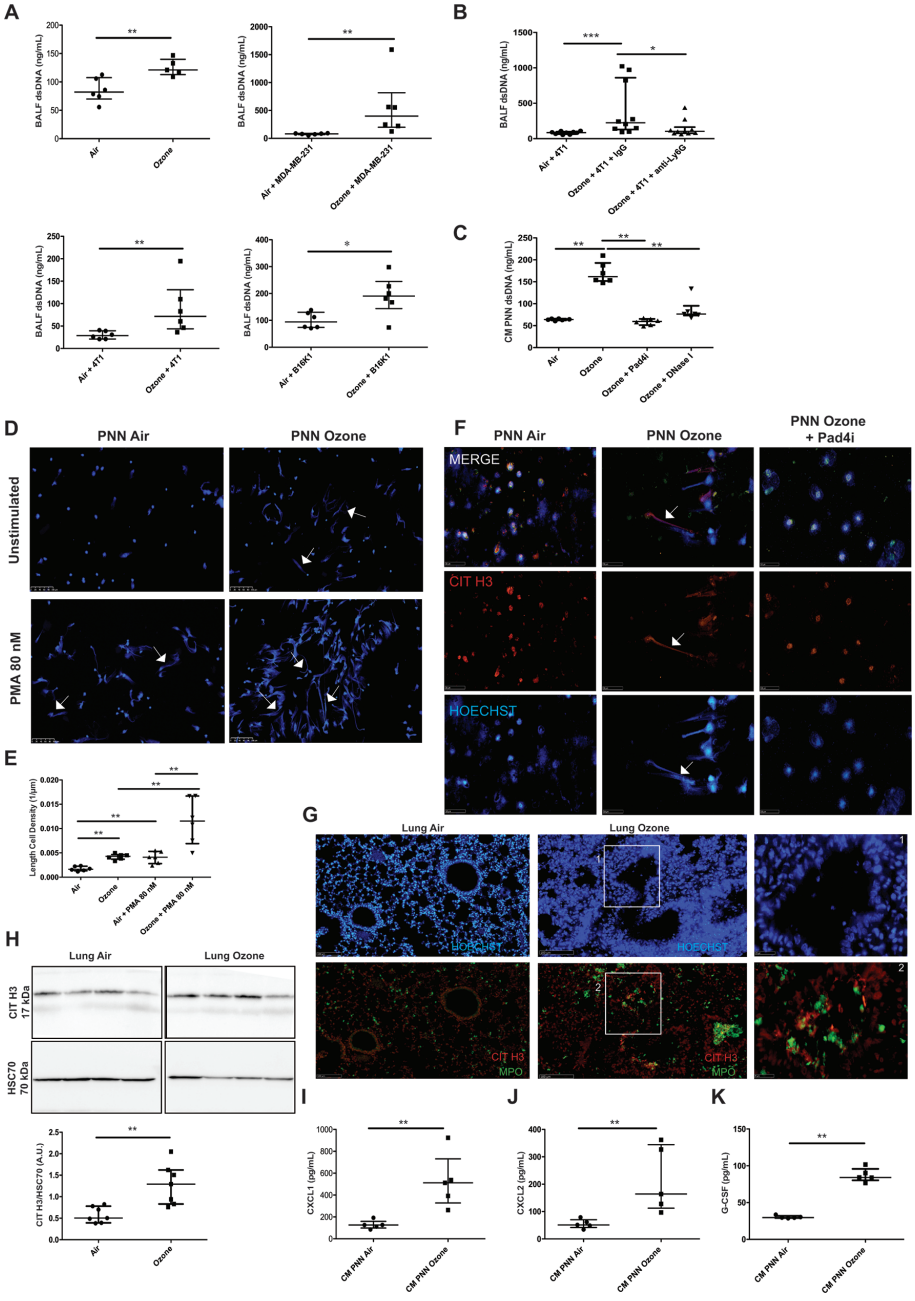

Figure 6 Ozone exposure activates neutrophils and triggers NET and chemokine production. (A) Levels of dsDNA measured in bronchoalveolar lavage fluids (BALF) of mice exposed to air or ozone, and injected with tumour cells (4T1, B16K1, MDA-MB-231) (*p<0.05; **p<0.01; Mann-Whitney test). Bars represent the IQR; n=6 mice/experimental group. (B) Levels of dsDNA measured in BALF of mice exposed to air (Air +4T1) or ozone, injected with 4T1 tumour cells and treated or not with the anti-Ly6G antibody (ozone +4T1+anti-Ly6G; ozone +4T1+IgG, respectively) (*p<0.05; ***p<0.001; Mann-Whitney test). Bars represent the IQR; n=9 (ozone +4T1+anti-Ly6G), 10 mice/experimental group. (C) Levels of dsDNA measured in media conditioned by ex vivo-cultured neutrophils (CM PNN) isolated from air-treated or ozone-treated lungs. Inhibitors of NET formation (Pad4i or DNase I) were used to treat ozone-stimulated neutrophils ex vivo. (**p<0.01; Mann-Whitney test). Bars represent the IQR; n=6 wells/experimental group. (D) Hoechst staining identifying NETs (white arrows) released by neutrophils derived from ozone-treated or air-treated lungs, stimulated or not with PMA (80 nM) (scale bar: 100 µm). (E) Computer-assisted quantification of length cell density. (**p<0.01; Mann-Whitney test). Bars represent the IQR; n=6 slides/experimental group. (F) Representative images of ex vivo-cultured neutrophils stained with anti-citrullinated histone 3 antibody (CIT H3 red) and Hoechst (blue) to identify NETs. A merge of all images is shown in the upper panel (scale bar: 50 µm); n=6 wells/condition. (G) Representative images of histological lung tissue sections stained with anti-CIT H3 (red), anti-MPO (green) antibodies and Hoechst (blue) to identify NETs (scale bar: 100 µm). For the ozone-treated group, a zoomed image is shown on the right (scale bar: 25 µm). n=5 lungs/experimental group. (H) CIT H3 levels (CIT H3, 17 kDa) have been quantified by western blot in protein extracts of air-treated and ozone-treated lungs. HSC70 (70 kDa) was quantified as loading control on the same blot. Lower panel shows graphic representation of densitometric quantification of CIT H3 and HSC70 staining. (**p<0.01; Mann-Whitney test). Bars represent the IQR; n=7 samples/experimental group. (I–K) ELISA analyses were performed to measure CXCL1, CXCL2 and G-CSF levels in supernatants conditioned by ex vivo-cultured neutrophils (CM PNN) previously isolated from air-treated or ozone-treated lungs (**p<0.01; Mann-Whitney test). Bars represent the IQR; n=5 samples/experimental group. G-CSF, granulocyte colony-stimulating factor; MPO, myeloperoxidase; NET, neutrophil extracellular trap; Pad4, peptidylarginine deiminase 4.

in supernatants of neutrophils extracted from ozone-stimulated lungs (**p<0.01, n=5) (figure 6I–K). Overall, these results indicate that neutrophils derived from ozone-treated lungs display a primed phenotype with increased production of chemokines and NETs.

To formally assess the contribution of NETs in metastatic processes in vivo, mice with neutrophil-specific *Pad4* deficiency (*Mrp8;Cre*$^{+}$*;Pad4*$^{fl/fl}$) or control wild type (WT) littermates were subjected to ozone and 4T1 tumour cell injection. Mice exhibiting *Pad4*-deficient neutrophils displayed decreased 4T1-related bioluminescent activity in lung regions as compared with WT littermates, already 24 hours after tumour cell injection, which persisted until 7 days after 4T1 injection (*p<0.05, n=5–8) (figure 7A–B). Tumour area quantification on H&E-stained histological lung sections confirmed these data (*p<0.05) (figure 7C). Moreover, mice exposed to ozone and treated on a daily basis with DNase I to denature NET meshes revealed an impaired metastatic development in lungs as from 24 hours after intravenous 4T1 cell injection as stated by biophotonic monitoring (*p<0.05) and tumour area quantification on histological lung tissue slides (**p<0.01, n=9) (figure 7D–F). These data clearly demonstrate the importance of NET production in early metastatic steps in vivo.

DISCUSSION

Air pollution has become a major public health problem and is now considered as a threat for susceptible individuals. In this context, epidemiological data clearly show that patients with lung and breast cancer exposed to air pollution have a poorer prognosis.[15–17]

Despite all efforts implemented to improve air quality, the air quality index still remains below hazardous levels in many major cities.[18] Hence, air pollution is responsible for millions of deaths and represents one of the leading risk factors for global disease burden in the world.[19] Ground-level ozone exposure has direct effects on lungs as it causes exacerbations of airway asthmatic diseases such as eosinophilic inflammation, airway hyperresponsiveness and mucus hyperproduction.[20–22] Yet, no bond between ozone-related inflammation and metastatic dissemination can be found in the literature.

In this experimental work, we describe for the first time a role for ozone exposure in the promotion of lung metastasis through the generation of a pulmonary neutrophilic inflammation and neutrophil-derived NETs. This evidence is supported by (1) The finding of an increased metastatic burden in lungs of mice exposed to ozone and intravenously injected with different tumour cell types, (2) Increased lung metastatic foci in ozone-challenged mice subcutaneously injected with tumour cells, (3) Prevention of ozone-induced metastasis after systemic depletion of neutrophils in mice, (4) The ability of ozone-primed neutrophils to enhance lung colonisation by tumour cells after adoptive transfer in mice unexposed to ozone. Based on our original data, we can further state that ozone and more precisely ozone-primed neutrophils modulate early events of the metastatic cascade since (1) Tumour cell dissemination to lungs was affected by ozone as soon as 30 min after intravenous tumour cell injection, (2) Neutralising neutrophil recruitment to lungs drastically reversed tumour cell spreading already 24 hours after tumour cell injection. One of the key findings of our study is that the adoptive transfer to lungs of neutrophils extracted from ozone-stimulated lungs or the instillation of supernatants collected after their ex vivo culture significantly increased tumour cell recruitment to lungs indicating that products secreted by ozone-challenged neutrophils account for the increased tumour cell dissemination. NET inhibition studies either with DNase I or by the use of animals bearing *Pad4*-deficient neutrophils strongly support the hypothesis that NETs, stimulated by ozone in mouse lungs or in ex vivo neutrophil cultures, trigger metastatic dissemination.

In our model, the implication of neutrophils in the metastatic process was supported by short-term and long-term in vivo Ly6G-depletion experiments. Clinical data evidently correlate neutrophil presence in tumours or in blood of patients with advanced cancer with poor prognosis.[23 24] However, contradictory roles have been attributed to neutrophils in tumour surveillance since cytotoxic and antimicrobial contents of their granules can destroy malignant cells and are responsible for antitumour responses.[25] To overcome this controversy, several reports specify that neutrophil functions vary with tumour progression stages.[26] In metastasis generation, neutrophils have been described to promote early metastatic events either by promoting tumour cell invasion, by facilitating the metastatic niche, or through matrix metalloproteinase 9 or interleukin 16 production.[27–29] Another key feature of neutrophils is their ability to produce NETs. These chromatin-based traps display the capacity to kill micro-organisms, are present in the sputum of patients with cystic fibrosis or COPD, where they contribute to tissue damage,[30] or in endobronchial biopsies of patients with asthma.[31] Moreover, NETs promote rhinovirus-induced allergic asthma exacerbations.[32] NETs can, by providing a scaffold to tumour cells, promote the arrest of circulating tumour cells,[33 34] increase vascular permeability[35] and participate in tumour cell expansion.[36] In the present study, increased dsDNA levels were detected in BALF of ozone-stimulated mice suggesting increased NET release in ozone-exposed lungs. Furthermore, evidence is provided that ozone-stimulated neutrophils produce higher NET levels ex vivo as compared with unstimulated neutrophils, while after PMA treatment, ozone neutrophils produce even higher amounts of NETs. In line with these results, recent data show that pulmonary cigarette-smoke exposure is not sufficient and needs PMA stimulation to induce ex vivo NET production by neutrophils.[37] Increased production of CXCL1, CXCL2 and G-CSF by ozone-primed neutrophils further supports our data of an ozone-driven activation of neutrophils.[38] Increased NET levels could account for the enhanced tumour cell dissemination observed in ozone-treated mice since neutrophils isolated from ozone-challenged lungs or media conditioned by these neutrophils highly induced tumour cell dissemination in naive mice. The reduced metastasis observed in mice exhibiting *Pad4*-deficient neutrophils, unable to release NETs, strongly supports our hypothesis. Altogether, these results underline the tremendous importance of ozone-primed neutrophils and derived extracellular traps in the control of metastatic steps. Our data have potential important clinical implications and contribute to explain the increased morbidity reported in patients with cancer living in polluted areas.[15–17 39] Although a bond between lung cancerisation and ozone exposure is expectable, the present data linking ozone with metastatic dissemination of mammary or melanoma cells indicate that in a personalised medicine perspective, one should certainly take into account environmental factors that might contribute to cancer progression and recommendations to patients might be helpful. On the other hand, it is not excluded that inhibition of NET formation in patients likely to develop lung metastasis could be a therapeutic option and could reduce adverse effects of environmental pollution.

Author affiliations
[1]Laboratory of Tumor and Development Biology, GIGA Research Center, Department of Biomedical and Preclinical Sciences, University of Liège, Liège, Belgium
[2]Laboratory of Cellular and Molecular Immunology, GIGA Research Center, University

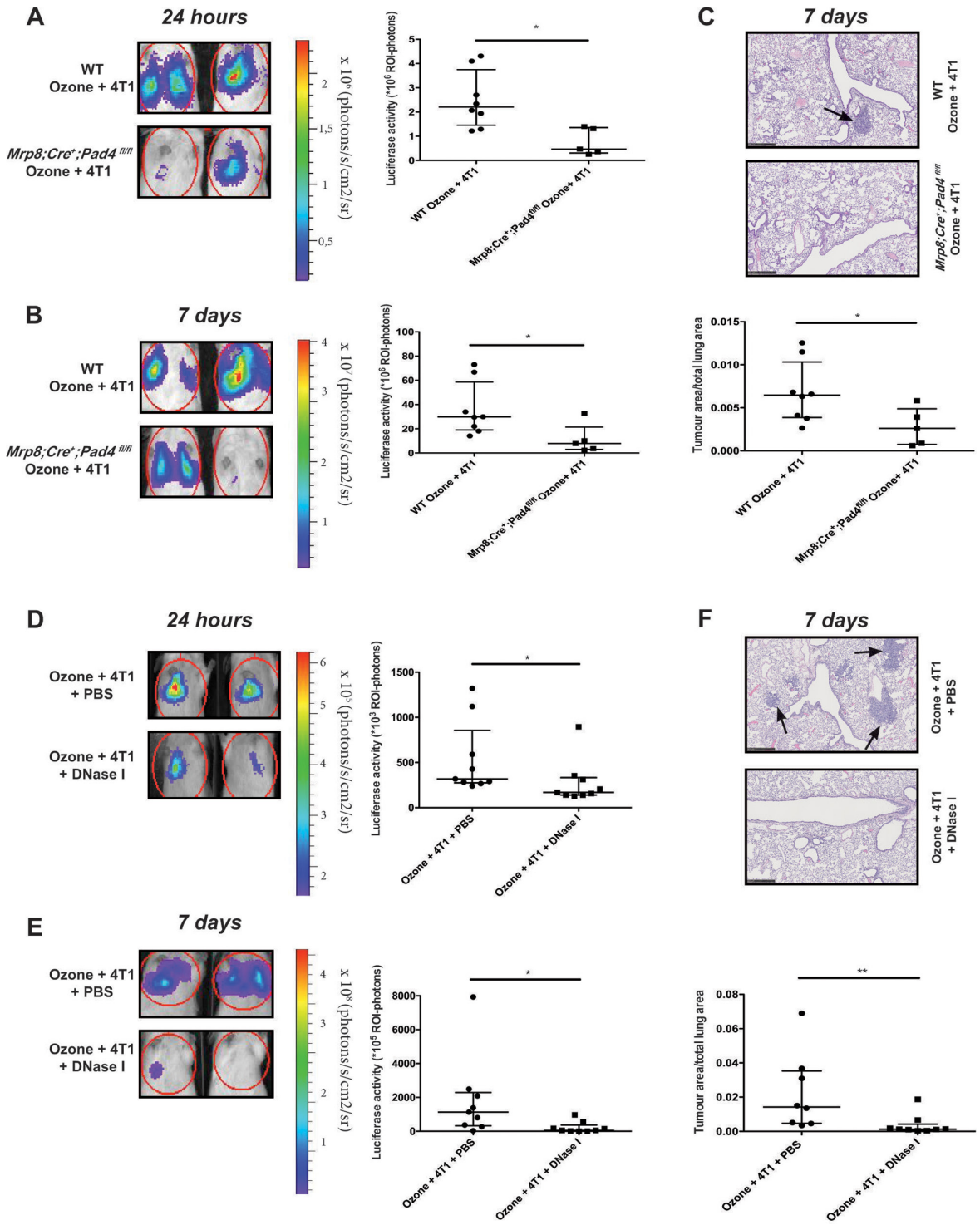

Figure 7 Lung metastasis onset is critically dependent on ozone-induced NETs. (A–B) Representative images of biophotonic luminescence measurements in lungs (red circles) of wild type (WT) or *Mrp8;Cre*$^{+}$*;Pad4*$^{fl/fl}$ mice 24 hours (A) and 7 days (B) after ozone exposure and intravenous 4T1 injection. Images have been taken in 'photon mode' and are representative of all mice analysed. The right panels show the quantification of luciferase-activity (photons) in regions of interest (ROI) (*p<0.05; Mann-Whitney test). Bars represent the IQR; n=5 mice for *Mrp8;Cre*$^{+}$*;Pad4*$^{fl/fl}$ and n=8 for the WT group. (C) Upper panel: representative H&E-stained histological lung tissue slides of WT or *Mrp8;Cre*$^{+}$*;Pad4*$^{fl/fl}$ mice. Black arrow shows tumour islet in lung tissues. Scale bar: 500 µm. Lower panel: the area occupied by tumours present in mouse lungs was quantified by measuring the ratio between tumour foci area and total area of analysed lungs (*p<0.05; Mann-Whitney test). Bars represent the IQR; n=5 mice for *Mrp8;Cre*$^{+}$*;Pad4*$^{fl/fl}$ and n=8 for the WT group. (D–E) Luciferase activity measurements 24 hours (D) and 7 days (E) after 4T1 tumour cell injection in mice exposed to ozone and treated or not with DNase I (Ozone +4T1+DNase I or Ozone +4T1+PBS, respectively). Quantification of luciferase activity is shown on the right (*p<0.05; Mann-Whitney test). Bars represent the IQR; n=9 mice/experimental group. (F) Upper panel: representative H&E-stained histological lung tissue slides of mice exposed to ozone, intravenously injected with 4T1 cells and intraperitoneally treated or not (phosphate buffer saline (PBS)) with DNase I. Black arrows show tumour islets in lung tissues. Scale bar: 500 µm. Lower panel: Tumour area quantification in mouse lung tissue sections. (**p<0.01; Mann-Whitney test). Bars represent the IQR; n=9. NET, neutrophil extracellular trap.

of Liège, Liège, Belgium
[3]Faculty of Veterinary Medicine, University of Liège, Liège, Belgium
[4]Montefiore Institute, Department of Electrical Engineering and Computer Science, University of Liège, Liège, Belgium
[5]Laboratory of Pharmaceutical Technology and Biopharmacy, Department of Pharmacy, Center for Interdisciplinary Research on Medicines (CIRM), University of Liège, Liège, Belgium
[6]WELBIO, Walloon Excellence in Life Sciences and Biotechnology, Wallonia, Belgium
[7]Respiratory Diseases, CHU Liège and University of Liège, Liège, Belgium

Acknowledgements The authors thank Christine FINK, Pascale Heneaux, Fabienne PERIN, Fanny Vaesen for technical support. The authors also acknowledge the GIGA-Mouse facility platform and the GIGA-Cell Imaging and Flow Cytometry platform (GIGA, University of Liège).

Contributors NR contributed to conception and design of the work, development of methodology, data collection, analysis interpretation, preparation of figures, and manuscript preparation and critical revision. CV contributed to development of methodology, data collection, analysis interpretation, preparation of figures and critical revision of the manuscript. CR gave technical support and expertise in NET experiments. SB contributed to image analysis and interpretation of results. CG helped in interpreting and validating results, guided the research strategy and critically revised the manuscript. RM supported the project by affording his expertise in quantifications of tumour sizes in histology. AG and BE critically revised the manuscript. CP provided B16K1 cells and critically revised the manuscript. TM provided expertise with NET experiments, generated and provided Mrp8;Cre+;Pad4fl/fl mice and critically revised the manuscript. AN contributed to project supervision, manuscript preparation and critically revised the manuscript. DC conceived the research program, applied to grants for funding, supervised experiments and manuscript revision, and submitted the manuscript to the editor.

Funding This study was financially supported by grants from the WB health program of the Walloon Region (WB Health AEROGAL, Convention n°1318023), the Fonds National pour la Recherche Scientifique (FRS-FNRS Télévie, Grant n°7463012F), the Centre AntiCancéreux (University of Liège), the Foundation against Cancer (foundation of public interest, Belgium), Interuniversity Attraction Poles Program-Belgian State-Belgian Science Policy-project P7/30 and the Fonds Léon Fredericq (University of Liège). NR is a research fellow of the Walloon Region (DGO6, WB Health AEROGAL, Convention n°1318023); RM is a research fellow of the Walloon Region (DGO6, Histoweb, grant n°1318185; Cytomine, grant n°1017072); CR was a research fellow of the F.R.S-FNRS; TM is a Research Associate of the F.R.S.-FNRS and is supported by an ERC Starting Grant (801823), an 'Incentive Grant for Scientific Research' of the F.R.S.-FNRS (F.4508.18), by the FRFS-WELBIO under grant CR-2017s-04 and by the Acteria Foundation.

Competing interests DC is the founder of Aquilon Pharmaceuticals, received speaker fees from AstraZeneca, Boehringer-Ingelheim, Novartis, MundiPharma, Chiesi and GSK and received consultancy fees from AstraZeneca, Boehringer-Ingelheim, and Novartis for the participation to advisory boards. None of these activities have any connection with oncology or development of drugs in the field of oncology.

Patient consent for publication Not required.

Provenance and peer review Not commissioned; externally peer reviewed.

Data availability statement All data relevant to the study are included in the article or uploaded as supplementary information.

REFERENCES

1 West R. Tobacco smoking: health impact, prevalence, correlates and interventions. *Psychol Health* 2017;32:1018–36.
2 Feys L, Descamps B, Vanhove C, *et al*. Radiation-induced lung damage promotes breast cancer lung-metastasis through CXCR4 signaling. *Oncotarget* 2015;6:26615–32.
3 Villeneuve PJ, Parent Marie-Élise, Sahni V, *et al*. Occupational exposure to diesel and gasoline emissions and lung cancer in Canadian men. *Environ Res* 2011;111:727–35.
4 Richters A, Kuraitis K. Air pollutants and the facilitation of cancer metastasis. *Environ Health Perspect* 1983;52:165–8.
5 Fridlender ZG, Sun J, Kim S, *et al*. Polarization of tumor-associated neutrophil phenotype by TGF-beta: "N1" versus "N2" TAN. *Cancer Cell* 2009;16:183–94.
6 de Torres JP, Marín JM, Casanova C, *et al*. Lung cancer in patients with chronic obstructive pulmonary disease-- incidence and predicting factors. *Am J Respir Crit Care Med* 2011;184:913–9.
7 Young RP, Hopkins R, Eaton TE. Forced expiratory volume in one second: not just a lung function test but a marker of premature death from all causes. *Eur Respir J* 2007;30:616–22.
8 Liang W, Ferrara N. The complex role of neutrophils in tumor angiogenesis and metastasis. *Cancer Immunol Res* 2016;4:83–91.
9 Hurt B, Schulick R, Edil B, *et al*. Cancer-promoting mechanisms of tumor-associated neutrophils. *Am J Surg* 2017;214:938–44.
10 Zhang X, Zhang W, Yuan X, *et al*. Neutrophils in cancer development and progression: roles, mechanisms, and implications (review). *Int J Oncol* 2016;49:857–67.
11 Albrengues J, Shields MA, Ng D, *et al*. Neutrophil extracellular traps produced during inflammation awaken dormant cancer cells in mice. *Science* 2018;361.
12 Pieterse E, Rother N, Garsen M, *et al*. Neutrophil extracellular traps drive endothelial-to-mesenchymal transition. *Arterioscler Thromb Vasc Biol* 2017;37:1371–9.
13 Kaplan MJ, Radic M. Neutrophil extracellular traps: double-edged swords of innate immunity. *J Immunol* 2012;189:2689–95.
14 Papayannopoulos V, Metzler KD, Hakkim A, *et al*. Neutrophil elastase and myeloperoxidase regulate the formation of neutrophil extracellular traps. *J Cell Biol* 2010;191:677–91.
15 Xu X, Ha S, Kan H, *et al*. Health effects of air pollution on length of Respiratory cancer survival. *BMC Public Health* 2013;13.
16 Eckel SP, Cockburn M, Shu Y-H, *et al*. Air pollution affects lung cancer survival. *Thorax* 2016;71:891–8.
17 Hu H, Dailey AB, Kan H, *et al*. The effect of atmospheric particulate matter on survival of breast cancer among US females. *Breast Cancer Research and Treatment* 2013;139:217–26.
18 Tanday S. India launches air quality index to tackle pollution problems. *Lancet Oncol* 2015;16:e203.
19 Lim SS, Vos T, Flaxman AD, *et al*. A comparative risk assessment of burden of disease and injury attributable to 67 risk factors and risk factor clusters in 21 regions, 1990–2010: a systematic analysis for the global burden of Disease Study 2010. *The Lancet* 2012;380:2224–60.
20 Duan L, Li J, Ma P, *et al*. Vitamin E antagonizes ozone-induced asthma exacerbation in BALB/c mice through the Nrf2 pathway. *Food Chem Toxicol* 2017;107:47–56.
21 Larsen SØren T., Matsubara S, McConville G, *et al*. Ozone increases airway hyperreactivity and mucus hyperproduction in mice previously exposed to allergen. *Journal of Toxicology and Environmental Health, Part A* 2010;73:738–47.
22 Kierstein S, Krytska K, Sharma S, *et al*. Ozone inhalation induces exacerbation of eosinophilic airway inflammation and hyperresponsiveness in allergen-sensitized mice. *Allergy* 2008;63:438–46.
23 Thålin C, Lundström S, Seignez C, *et al*. Citrullinated histone H3 as a novel prognostic blood marker in patients with advanced cancer. *Plos One* 2018;13:e0191231.
24 Wang J, Jia Y, Wang N, *et al*. The clinical significance of tumor-infiltrating neutrophils and neutrophil-to-CD8+ lymphocyte ratio in patients with resectable esophageal squamous cell carcinoma. *Journal of Translational Medicine* 2014;12.
25 Völs S, Sionov RV, Granot Z. Always look on the bright side: anti-tumor functions of neutrophils. *Curr Pharm Des* 2017;23:4862–92.
26 Mishalian I, Bayuh R, Levy L, *et al*. Tumor-associated neutrophils (Tan) develop pro-tumorigenic properties during tumor progression. *Cancer Immunology, Immunotherapy* 2013;62:1745–56.
27 Huh SJ, Liang S, Sharma A, *et al*. Transiently entrapped circulating tumor cells interact with neutrophils to facilitate lung metastasis development. *Cancer Research* 2010;70:6071–82.
28 Uribe-Querol E, Rosales C. Neutrophils in cancer: two sides of the same coin. *Journal of Immunology Research* 2015;2015:1–21.
29 Donati K, Sépult C, Rocks N, *et al*. Neutrophil-derived interleukin 16 in Premetastatic lungs promotes breast tumor cell seeding. *Cancer Growth and Metastasis* 2017;10.
30 Grabcanovic-Musija F, Obermayer A, Stoiber W, *et al*. Neutrophil extracellular trap (NET) formation characterises stable and exacerbated COPD and correlates with airflow limitation. *Respiratory Research* 2015;16.
31 Dworski R, Simon H-U, Hoskins A, *et al*. Eosinophil and neutrophil extracellular DNA traps in human allergic asthmatic airways. *Journal of Allergy and Clinical Immunology* 2011;127:1260–6.
32 Toussaint M, Jackson DJ, Swieboda D, *et al*. Host DNA released by NETosis promotes rhinovirus-induced type-2 allergic asthma exacerbation. *Nature Medicine* 2017;23:681–91.
33 Erpenbeck L, Schön MP. Neutrophil extracellular traps: protagonists of cancer progression? *Oncogene* 2017;36:2483–90.
34 Papayannopoulos V. Neutrophil extracellular traps in immunity and disease. *Nature Reviews Immunology* 2017;18:134–47.
35 Kolaczkowska E, Jenne CN, Surewaard BGJ, *et al*. Molecular mechanisms of net formation and degradation revealed by intravital imaging in the liver vasculature. *Nature Communications* 2015;6.
36 Park J, Wysocki RW, Amoozgar Z, *et al*. Cancer cells induce metastasis-supporting neutrophil extracellular DNA traps. *Science Translational Medicine* 2016;8.
37 Qiu S-L, Zhang H, Tang Q-Y, *et al*. Neutrophil extracellular traps induced by cigarette smoke activate plasmacytoid dendritic cells. *Thorax* 2017;72:1084–93.
38 Nguyen-Jackson HT, Li HS, Zhang H, *et al*. G-CSF-activated Stat3 enhances production of the chemokine MIP-2 in bone marrow neutrophils. *J Leukoc Biol* 2012;92:1215–25.
39 Ancona C, Badaloni C, Mataloni F, *et al*. Mortality and morbidity in a population exposed to multiple sources of air pollution: a retrospective cohort study using air dispersion models. *Environ Res* 2015;137:467–74.